Correcting for H_2O interference using a RAD7 electrostatic collection-based silicon detector

G. De Simone [a], C. Lucchetti [a], G. Galli [b], P. Tuccimei [a, *]

[a] *Università "Roma Tre", Dipartimento di Scienze, Largo San Leonardo Murialdo 1, 00146 Roma, Italy*
[b] *Istituto Nazionale di Geofisica e Vulcanologia, Sezione Roma 1, Via di Vigna Murata 605, 00143, Roma, Italy*

ABSTRACT

The effect of water molecules on the electrostatic collection of ^{218}Po ions onto the surface of silicon detectors (neutralization) is evaluated through the comparison with a scintillation cell (ZnS), not affected by air humidity. A radon monitor (RAD7, Durridge Company) was connected to a stainless steel radon chamber, equipped with the scintillation cell. Radon gas, extracted from an acidified $RaCl_2$ source, was injected into the chamber and the amount of water molecules in the system was alternatively lowered or increased (from 0.00075 to 0.014 g of water in RAD7) by connecting the chamber to a desiccant or to a bubbling water bottle. The relative efficiency of the silicon detector with respect to the scintillation cell decreases with the growth of water molecules inside RAD7. This dependence, with a fixed *i*) electrostatic chamber geometry and *ii*) nominal high voltage, diverges during the humidification or the drying phase because it is in turn influenced by the length of interaction of polonium atoms with water molecules, which impacts on the size of ^{218}Po clusters and thus on the neutralization process. For water contents higher that 0.01 g in RAD7, this effect is greatly enhanced. Temperature in the investigated range (18.5 – 35.6°C) does not affect the efficiency of electrostatic collection-based silicon detectors.

Based on these experiments, admitting a certain error on the efficiency (from 1.8 to 7.5 %, depending on the water content), proper corrections were developed to adjust soil radon readings, when a desiccant is removed. This operation is necessary if recent Non-Aqueous Phase Liquids (NAPLs) leakage has occurred in the subsoil to avoid the sorption and possible later release of radon by Drierite, with related partition between the solid and liquid phases (water and NAPL).

Keywords:
Soil radon
RAD7
Scintillation cell
^{218}Po neutralization by water vapor
NAPL contamination

* Corresponding author.
E-mail address: paola.tuccimei@uniroma3.it (P. Tuccimei)

1. Introduction

Radon is a radioactive gas naturally present in the environment at different levels. It reaches highest activity concentration in the subsoil and in groundwater, whereas it is less abundant at the surface. Radon may accumulate inside edifices built on radon precursors-enriched geological bedrocks, especially during cold and rainy periods, when the climate favours radon accumulation in the soil and its migration to indoor environments. Long exposure to indoor radon increases the risk of lung cancer, especially for smokers and people exposed to second hand smoke (EPA, 2003). Consequently, assessment of health risks and mitigation actions of edifices are required, either from indoor radon or in-soil radon data.

Among methods routinely employed to detect radon in the environment, those based on solid state silicon detectors and radon (^{222}Rn and ^{220}Rn) daughters electrostatic collection (Chao et al., 1997; De Martino et al., 1998; Roca et al., 2004; Tuccimei et al., 2006; Lucchetti et al., 2016) are very frequently used. It is well known that their counting efficiency is influenced by environmental parameters such as humidity, temperature and pressure (Chu and Hopke, 1988; Hopke, 1989; Roca et al., 2004; Tuccimei et al., 2006). Temperature and water content in soil gas affect these measurements because water molecules in the counting chambers of radon monitors cause the neutralization of radon progenies, reducing the electrostatic efficiency of silicon detector. Desiccants such as calcium sulphate (Drierite) are employed to reduce this effect, but during humid summer time it is difficult to dry efficiently soil gas and the interference from water molecules needs to be corrected for.

Radon is also used as tracer for environmental processes (Quindos et al., 2013), such as: indicator of atmospheric dynamics (Cuculeanu and Lupu, 2013); precursor of rock deformation and degassing phenomena in volcanic settings (Tuccimei et al., 2010; Scarlato et al., 2013); tracer of groundwater discharge into rivers (Cook et al., 2003), coastal ocean (Cable et al., 1996) or surface reservoirs (Corbett et al., 1997); for the assessment of residual NAPLs (Non-Aqueous Phase Liquids) contamination of soils and aquifers (Semprini et al., 2000; Schubert et al., 2002; Schubert, 2015).

In order to use radon as NAPL tracer, we investigated if Drierite interferes with NAPLs in contaminated soil. Proper experiments were carried out in laboratory repeatedly connecting in a closed loop a RAD7 instrument, a Drierite column previously polluted with NAPL vapors and a small radon chamber (2.83 L) with a fixed activity of radon (see Fig. 1): at the end of each test, after measuring the equilibrium radon concentration, a partial purging of the RAD7 and the Drierite column was performed for a time of 5 minutes, not long enough to remove completely the absorbed NAPL. Since radon concentration is expected to decrease in successive experiments for decay and dilution, this process has been accounted for; nonetheless we observed firstly a decrease (28%) with respect to the expected value, then successive experiments showed progressive increases of radon concentrations (16 and 23%). As a matter of fact, firstly, NAPL vapor absorbed in the Drierite captures radon (test 2), reducing its concentration in the circuit;

successive experiments (test 3 and 4) showed that NAPL still absorbed in the Drierite column is partially released to the closed loop, leading to a consequent rise of radon in the circuit.
Accordingly, when soil radon measurements are carried out in presence of recent NAPLs contamination (De Simone et al., 2015a), these substances are extracted during soil gas sampling and then absorbed by desiccant material, partitioning radon gas between the air and the absorbed liquid phases (the NAPL and the water). This leads to an interference difficult to deal with and thus desiccants should be removed.
This is why we developed proper experiments to correct radon concentration detected by RAD7 electrostatic collection-based silicon detectors for the weight of water molecules in the system.

2. Material and Methods

Radon activity concentration was measured using a RAD7 monitor (Durridge Co.), an electrostatic chamber operated at a nominal voltage of 2,000 – 2,500 V, equipped with a solid state silicon detector which collects radon daughters onto its surface and detects and separates alpha particles emitted by them, on the basis of their energies. This allows to select only the short-lived ^{218}Po (with a half-life of about 3 minutes) to measure ^{222}Rn, reaching the radioactive equilibrium between them in just 15 minutes. This option (the Sniff mode, according to RAD7 protocols) allows to change experimental conditions fast and perform the test relatively rapidly. In order to reduce the water content in the counting chamber of the instrument, a cylinder of calcium sulphate (Drierite) is generally employed. Temperature and relative humidity are recorded inside the instrument. A pump guarantees the circulation of the air in the set-up.
Radon concentration in the radon chamber was determined with a scintillation cell (ZnS) coupled to a photomultiplier (De Simone et al., 2015b) to have radon reference values not affected by changing water conditions, as described in the following sections.

3. Experimental

In order to obtain the dependence of decreased detection efficiency of the RAD7 silicon detector on absolute humidity, ad-hoc experiments were designed using a 56 L stainless steel radon chamber equipped with a scintillation cell (ZnS) coupled to a photomultiplier, which is not sensitive to humidity. Radon gas was extracted from an acidified (pH< 2) $RaCl_2$ source added with Ba (2,500 Bq), and injected in the chamber. Relative humidity and thus weight of water molecules in the system, at constant temperature, were progressively changed by connecting the chamber to Drierite (opening stopcocks O and Q and closing stopcocks P and R) or to a bubbling water bottle (opening stopcocks O and R and closing stopcocks P and Q) for drying or humidifying the closed circuit. When reached desired condition, RAD7 was connected in a closed loop to the chamber (opening stopcock P and closing stopcocks O, Q and R) and RAD7 readings were compared with activity concentrations given by the scintillator at each step (with an average duration of 30-45 minutes per step) (Fig. 2). It is worth noting that the scintillator data used for efficiency calculation were always obtained from an exponential interpolation of counts recorded after at least 5 hours from the RAD7 connection to the radon chamber, to account for the establishment

of new equilibrium conditions (secular equilibrium and radon diffusion within the new system configuration) and to reduce the error.
A number of experiments were carried out according to a planned sequence of drying or humidification phases in order to study the repeatability and the dependence of results on the sequence path. As a result, correction factors of activity concentration values obtained using RAD7 (defined as efficiency of the electrostatic collection-based silicon detector) were calculated as the ratio:

$$Efficiency_{\ i} = A_{Rn\ RAD7\ i} / A_{Rn\ CR\ i} \qquad eq.\ 1$$

and plotted versus the amount of water in the RAD7, being $A_{Rn\ RAD7\ i}$ the i-th average radon activity concentration measured by the RAD7 (printed raw readings) in each step and $A_{Rn\ \ CR\ \ i}$ the corresponding i-th radon activity concentration in the radon chamber.
Each $A_{Rn\ CR}$ was calculated by exponential interpolation ($A_{Rn\ CR} = k*Y_0*e^{B*t}$) obtained as described above, of data registered by a multichannel analyzer set in multiscaler mode, during each experiment configuration, where:

k: calibration factor (Bq m^{-3} cpm^{-1})
Y_0: counts (cpm) at t = 0
B: exponential time constant (min^{-1})
t: time (min)

Absolute humidity values in the detection volume, expressed as grams of water inside RAD7 (gH_2O_{RAD7}), are inferred from the psychrometric diagram as a function of the atmospheric pressure, temperature and relative humidity and calculated using equation 2:

$$gH_2O_{RAD7} = kgH_2O\ /\ Kg\ dry\ air\ *\ 1000\ *\ \rho\ air_{\ T}\ *\ V_{RAD7} \qquad eq.\ 2$$

where:
$kgH_2O\ /\ Kg\ dry\ air$: kilograms of water contained in a kilogram of dry air
$\rho\ air_{\ T}$: air density at a given temperature (kg/m^3)
V_{RAD7}: inner volume of RAD7 monitor (0.000768 m^3)

with
$$kgH_2O\ /\ Kg\ dry\ air = (0.622\ *\ RH/100\ *\ P_{sat}\ )\ /\ P - (RH/100\ *\ P_{sat}) \qquad eq.\ 3$$
(Gatley, 2013)

where:
RH: relative humidity
P_{sat}: water saturation pressure at a given temperature (Pa)
P: atmospheric pressure (Pa)

The water saturation pressure is calculated as follows:

$P_{sat} = exp\ [65.81 - 7066.27/(T + 273{,}17) - 5.976\ ln\ (T + 273.159)]$ *eq. 4*
(Gatley, 2013)

with
T = temperature in °C

The atmospheric pressure effect can be considered negligible, since a 10 mBar difference affects the water content for just 1 %, being the 1 sigma uncertainties on water content greater.

4. Results and discussion

It is known that water molecules dispersed in air reduce the collection of positively charged radon daughters on the silicon detector surface placed in an electrostatic chamber operated at constant nominal high voltage (HV). Electric field lines, oriented as shown in Fig. 3, influence not only the collection of the radon daughters, but also the trajectory of water-polonium clusters, which may hit the detector even though partly neutralized (Chu and Hopke, 1988; Hopke, 1989; Mesbah et al., 1997; De Martino et al., 1998; Roca et al., 2004; Tuccimei et al., 2006).
Proper experiments were carried out to assess the correction factor (efficiency) trend as a function of the water content inside a RAD7 (Serial Number, S.N. 2408) by using the experimental apparatus reported in Fig. 2. The water content was changed from 0.00075 to 0.014 g (approximately from 5 to 69 % relative humidity at about 26 ± 1 °C).

All the obtained efficiency values are plotted in Fig. 4 versus the water content inside RAD7 along with a linear interpolation for water contents < 0.010 g H_2O. The correction provided by Capture, the software developed by Durridge Co. for data acquisition and analysis, is also reported; the fit has been obtained from the ratios between raw and Capture corrected data. Capture correction agrees with the experimental data obtained from RAD7 (S.N. 2408) up to about 0.003 g H_2O in RAD7 volume; for higher water contents it underestimates the correction.
With reference to our experimental data, we note a decrease of the efficiency at increasing water contents due to neutralization processes; it is also evident that the higher the water content, the higher the scatter of efficiency data, especially observed during drying phases; furthermore, efficiency values obtained during drying starting from wet conditions generally lay below those obtained during humidification starting from dry conditions, this being very evident over 0.010 g H_2O in RAD7.
In order to highlight this, plots of efficiency data for water contents less than 0.010 g H_2O are shown in Fig. 5, (selecting data obtained during humidification) and in Fig. 6 (choosing data from drying), along with the linear interpolation equations.
The trend in Fig. 5 is more regular since the test starts from dryer conditions, definitely more suitable for the use of RAD7, as recommended by Durridge (Durridge, 2009). Fig. 6, reporting experimental data starting from wet conditions, shows a slightly different trend with a higher scatter at higher values of water. Finally, Fig. 7 refers to linear fits of data acquired during drying

and humidifying for water contents greater than 0.010 g H_2O; in this case the trends are clearly different and the experiment history must be accounted for, since water molecules deposited over the silicon detector surface cause an even stronger degradation in the detected alpha particles energy and consequently their removal from the ^{218}Po peak.

This is also evident in the case of Fig. 8 in which, during drying, theoretical efficiency data from interpolation in Fig. 6 are compared with experimental efficiency data: the latter at the beginning lay below the former and progressively approach them since the water molecules attached to the system walls (including the detector surface) are being removed along with the water-polonium clusters.

Finally, the temperature effect on the RAD7 response has been investigated. Consequently a specific experiment has been carried out at a water content nearly constant, varying greatly the temperature from 18.5 °C to 35.6 °C (see Fig. 9). The plot in Fig. 9a shows experimental efficiency data superimposed on the available data set (Fig. 4) from 0.005 to 0.008 g H_2O in RAD7 and the related interpolation fit. Data from this experiment, plotted versus the water content, follow reasonably the available data set, apart from an initial 10% deviation (average value of 6%) for low absolute humidity. According to what evidenced before, efficiency data from this experiment have been plotted (Fig. 9b) along with temperature and water content versus the chronological measure identification: again interpolated data are approached only after a time needed for the system equilibrium to be reached, i.e. water removal from the detector. As a matter of fact, initial efficiency values are about 11% lower than corrected efficiency (average value of 7%) in agreement with Fig. 9a. Therefore the temperature dependence must be evaluated only after correcting the data set for a factor depending from the initial disequilibrium (ratio between experimental and interpolated efficiency). Adjusted data follow the trend obtained varying the absolute humidity while keeping almost constant the temperature (Fig. 5); therefore the dependence of the RAD7 response from temperature is negligible.

Results obtained performing various experiments showed that the corrective factor depends on *i*) the amount of water in the detection volume, *ii*) the history of the measurements done, i.e. increasing water content starting from dry conditions or vice versa. The following linear interpolation equations have been found:

$Y = 1$	for X (g H_2O) < 0.00075 (Guantario, 1997; Durridge, 2009)	*eq. 5*
$Y = (-68.999 \pm 0.771)\,X + (1.052 \pm 0.005)$	for 0.00075<X (g H_2O)<0.010, all data	*eq. 6*
$Y = (-63.485 \pm 1.344)\,X + (1.047 \pm 0.008)$	for 0.00075<X (g H_2O)<0.010, humidifying only	*eq. 7*
$Y = (-70.715 \pm 1.037)\,X + (1.053 \pm 0.006)$	for 0.00075<X (g H_2O)<0.010, drying only	*eq. 8*
$Y = (-38.903 \pm 7.474)\,X + (0.840 \pm 0.087)$	for 0.010<X (g H_2O)<0.014, humidifying only	*eq. 9*
$Y = (-21.323 \pm 4.573)\,X + (0.558 \pm 0.055)$	for 0.010<X (g H_2O)<0.014, drying only	*eq. 10*

In any case, even *i*) ignoring the history effect and consequently the time required for the recovery of the full efficiency of electrostatic collection and *ii*) using the linear interpolation of all available data (Fig. 5), radon concentration values can be still inferred also in very critical conditions (water

contents up to 0.010 g H_2O in the RAD7). For example, the following average deviations from the corrected efficiency values have been calculated:
- g H_2O < 0.004 : 1.8%
- 0.004 < g H_2O < 0.007 : 4.1%
- 0.007 < g H_2O < 0.010 : 7.5%.

Finally, we tested with the same experimental setup also the other RAD7s (S.N. 0608 and 2504) we generally employ in field surveys, to verify whether their responses were similar to that obtained for RAD7 S.N. 2408. Results are summarized in Table 1.
Efficiency data are very different; efficiency relative deviations have been calculated with respect to RAD7 S.N. 2408. Deviation of RAD7 S.N. 0608 is about 14% higher, irrespective of the water content (0.004 – 0.014 gH_2O); deviation of RAD7 S.N. 2504 is again higher and ranges from 23% to 57% at increasing water contents.
Results demonstrate that corrections are different for each RAD7 since they depend even on small differences among instruments regarding *i*) detection chamber, *ii*) silicon detector, *iii*) temperature and RH sensors, *iv*) applied high voltage, *v*) pump volume rate, *vi*) electronics and *vii*) assembly.
A comparison with Capture correction shows that deviations from all investigated RAD7s are very different and generally increase with water contents; therefore each RAD7 must be characterized when not used according to the manufacturer recommendation, i.e. without Drierite. Capture correction works very well for every instrument up to 0.003 g H_2O in RAD7, corresponding for example to RH = 15% at 25°C, even beyond the recommended limit (RH < 10% at ambient temperature).

5. Conclusions

Soil radon is actually used as tracer of NAPLs contamination in the vadose zone of aquifers because it is more soluble in NAPLs than in water or in air and a deficit of it in soil gas (known as soil radon deficit technique, Semprini et al., 2000) pinpoints the volume of polluted subsoil. The use of desiccants to dry soil air interferes with the residual NAPL vapor, absorbing it and partition radon between the solid and the liquids. In further measurements carried out with the same Drierite column, without changing or purging it completely, NAPL vapors still absorbed onto the column may be released to the system, heavily affecting results (De Simone et al., 2015a).
As a consequence the use of Drierite should be avoided, irrespective of manufacturer recommendation, and proper correction for the efficiency of RAD7 electrostatic-based silicon detectors must be applied to account for the effect of water molecules on the electrostatic collection of ^{218}Po ions. Ad-hoc corrections have been obtained for a specific RAD7 at different water contents. The temperature influence has been ruled out.
Various RAD7s have been tested showing different behavior at similar water content, making the characterization of every single instrument necessary. Capture correction agrees with our experimental data up to 0.003 gH_2O in RAD7 volume, diverging progressively at increasing water contents.

References

Cable, J.E., Burnett, W.C., Chanton, J.P., Weatherly, G.L., 1996. Estimating groundwater discharge into the northeastern Gulf of Mexico using radon-222. Earth Planet. Sci. Lett. 144, 591–604.

Chao, C.Y.H., Tung, T.C.W., Chan, D.W.T., Burnett, J., 1997. Determination of radon emanation and back diffusion characteristics of building materials in small chamber tests. Build. Environ. 32, 355–362.

Chu, K-D., Hopke, P.K., 1988. Neutralization Kinetics for Polonium-218. Envir. Sci. Tech. 22, 711-717.

Cook, P.J., Favreau, G., Dighton, J.C., Tickell, S., 2003. Determining natural groundwater influx to a tropical river using radon, chlorofluorocarbons and ionic environmental tracers. J. Hydrol. 277, 74–88.

Corbett, D.R., Burnett, W.C., Cable, P.H., Clark, S.B., 1997. Radon tracing of groundwater input into Par Pond, Savannah River Site. J. Hydrol. 203, 209–227.

Cuculeanu, V., Lupu, A., 2001. Deterministic chaos in atmospheric radon dynamics. Deterministic chaos in atmospheric radon dynamics. J. Geophys. Res.-Atmos. 106, 961-968.

De Martino, S., Sabbarese, C., Monetti, G., 1998. Radon emanation and exhalation rates form soils measured with an electrostatic collector. Appl. Radiat. Isot. 49, 407–413.

De Simone, G., Galli, G., Lucchetti, C., Tuccimei P., 2015a. Using natural radon as a tracer of gasoline contamination. P. Earth Planet. Sci. 13, 104 – 107. 11th Applied Isotope Geochemistry Conference, AIG-11 BRGM.

De Simone, G., Galli, G., Lucchetti, C., Tuccimei P., 2015b. Calibration of BIG Bottle RAD H2O set-up for radon in water using HDPE bottles, Radiat. Meas. 76, 1-7.

(EPA) Environmental Protection Agency, 2003. EPA Assessment of Risks from Radon in Homes. 402-R-03-003. U.S. Environmental Protection Agency, Washington, DC, 2003.

Gatley, D.P., 2013. Understanding Psychrometrics. ASHRAE, third ed., Atlanta (GA), USA. ISBN 978-1-936504-31-2

Guantario, C., 1997. Influenza dell'umidità sulla efficienza di rivelazione di radon mediante rivelatore allo stato solido. Tesi di Laurea in Ingegneria Nucleare, Università "La Sapienza", Roma, Italy.

Hopke, P.K., 1989. Use of electrostatic collection of ^{218}Po for measuring Rn. Health Phys. 57, 39-42.

Lucchetti C., De Simone G., Galli G., Tuccimei P., 2016. Evaluating radon loss from water during storage in standard PET, bio-based PET and PLA bottles. Radiat. Meas., 84, 1-8.

Mesbah, B. Fitzgerald, B., Hopke, P. K., Pourprix, M., 2015. New technique to measure the mobility size of ultrafine radioactive particles. Aerosol Sci. Tech., 27, 381-393.

Quindos, L. S., Sainz, C., Fuente, I., Gutierrez J.L., Gonzalez, A., 2013. The Use of Radon as Tracer in Environmental Sciences. Acta Geophys., 61, 848-858.

Roca, V., De Felice, P., Esposito, A.M., Pugliese, M., Sabbarese, C., Vaupotich, J., 2004. The influence of environmental parameters in electrostatic cell radon monitor response. Appl. Radiat. Isot. 61, 243–247.

Scarlato P., Tuccimei P., Mollo S., Soligo M., Castelluccio M., 2013. Contrasting radon background levels in volcanic settings: clues from ^{220}Rn activity concentrations measured during long-term deformation experiments. B. Volcanol., 75:751, DOI 10.1007/s00445-013-0751-0.

Schubert, M., Freyer, K., Treutler, H.C., Weiss, H. 2002. Using radon-222 in soil gas as an indicator of subsurface contamination by non-aqueous phase liquids (NAPLs). Geofis. Int., 41, 433-437.

Schubert, M. 2015. Using radon as environmental tracer for the assessment of subsurface Non-Aqueous Phase Liquid (NAPL) contamination – A review. Eur. Phys. J. Special Topics 224, 717–730.

Semprini, L., Hopkins, O.S., Tasker, B.R., 2000. Laboratory, field, and modeling studies of Radon-222 as a natural tracer for monitoring NAPL contamination. Transport Porous Med., 38, 223-240.

Talbot, D.K., Appleton, J.D., Ball, T.K., Strutt, M.H., 1998. A comparison of field and laboratory analyticals methods for radon site investigation. J. Geochem. Explor. 65, 79–90.

Tuccimei, P., Moroni, M., Norcia. D., 2006. Simultaneous determination of ^{222}Rn and ^{220}Rn exhalation rates from building materials used in Central Italy with accumulation chambers and a continuous solid state alpha detector: Influence of particle size, humidity and precursors concentration. Appl. Radiat. Isot. 64, 254–263.

Tuccimei P., Mollo S., Vinciguerra S., Castelluccio M. , Soligo M., 2010. Radon and thoron emission from lithophysae-rich tuff under increasing deformation: an experimental study. Geophys. Res. Lett., 37, L05406, doi:10.1029/2009GL041652, 12 March 2010.

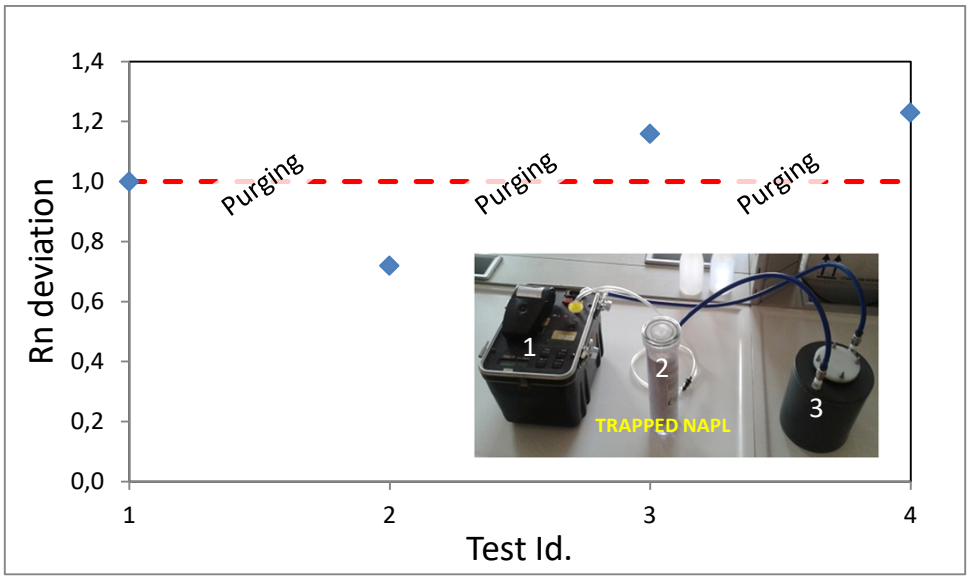

Fig. 1. Radon deviation from expected values when NAPL vapors are trapped into the Drierite column (2) in successive tests. 1) RAD7; 3) Small radon chamber. See text for explanation.

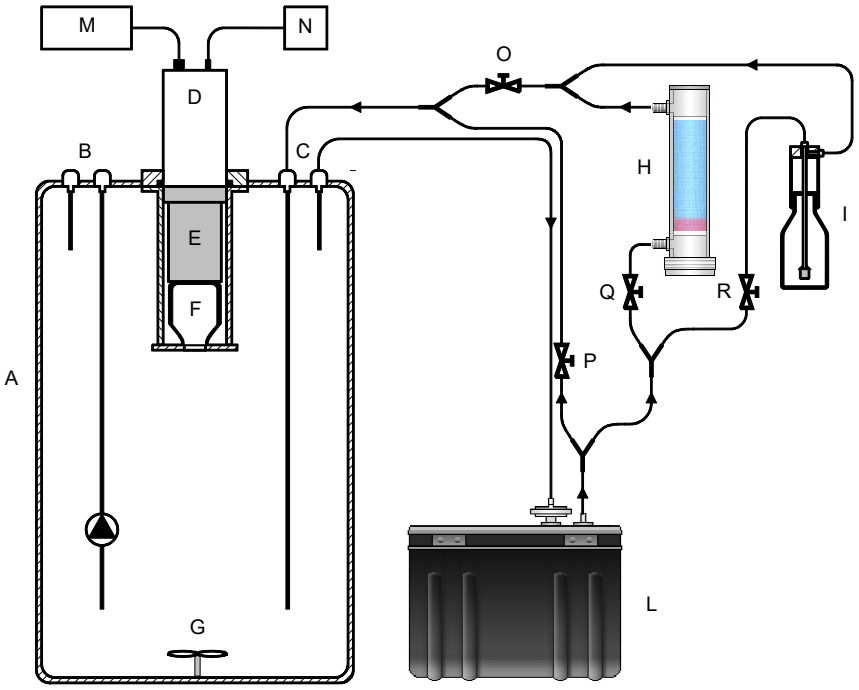

Fig. 2. Experimental set-up. A) radon chamber; B) air tight connectors (CPC) to be used when air circulation needs a pump; C) air tight connectors (CPC) when air circulation is guaranteed by an outer device; D) signal processing module; E) photomultiplier; F) scintillating flask; G) fan; H) desiccant column (Drierite); I) humidifying device; L) Durridge RAD7; M) multiscaler, N) low voltage supply; O), P), Q) and R) stopcocks.

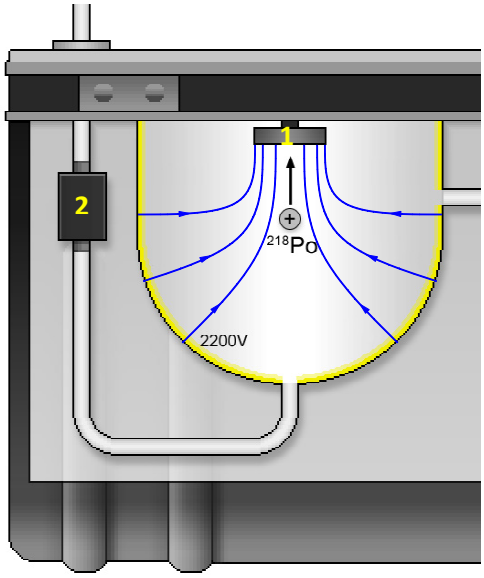

Fig. 3. Electric field lines in the counting chamber of RAD7. 1) solid-state, ion-implanted, planar, silicon alpha detector, 2) Temperature/Relative Humidity sensors. The scheme was kindly provided by Durridge Co.

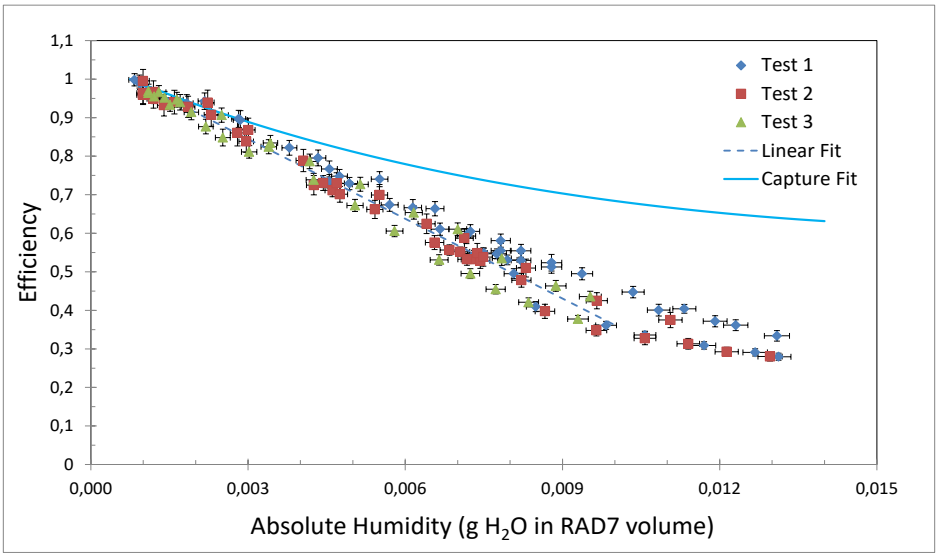

Fig. 4. Efficiency of the electrostatic collection-based silicon detectors against the water content inside RAD7 from three different experiments. The linear fit of all data up to 0.01 g of water in RAD7 volume is reported for comparison with figures 5, 6 and 7 where data are selected based on the degree and the changing trend of absolute humidity (humidification or drying). The solid line represents the correction given by Capture (see text for explanation).

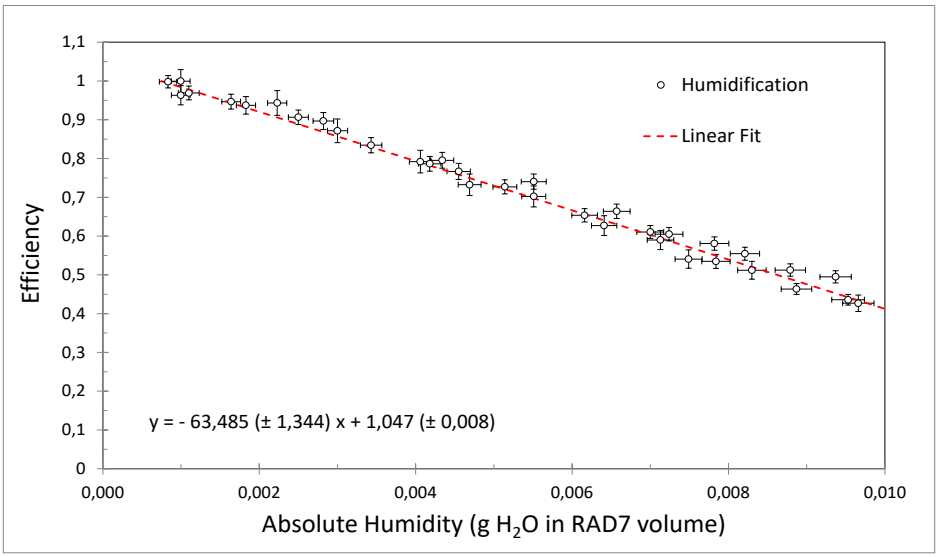

Fig. 5. Efficiency of the electrostatic collection-based silicon detectors against the water content inside RAD7. Data from the humidification phases of the three different experiments up to 0.01 g of water in RAD7 volume are selected. The linear fit is reported for comparison with figures 4, 6 and 7.

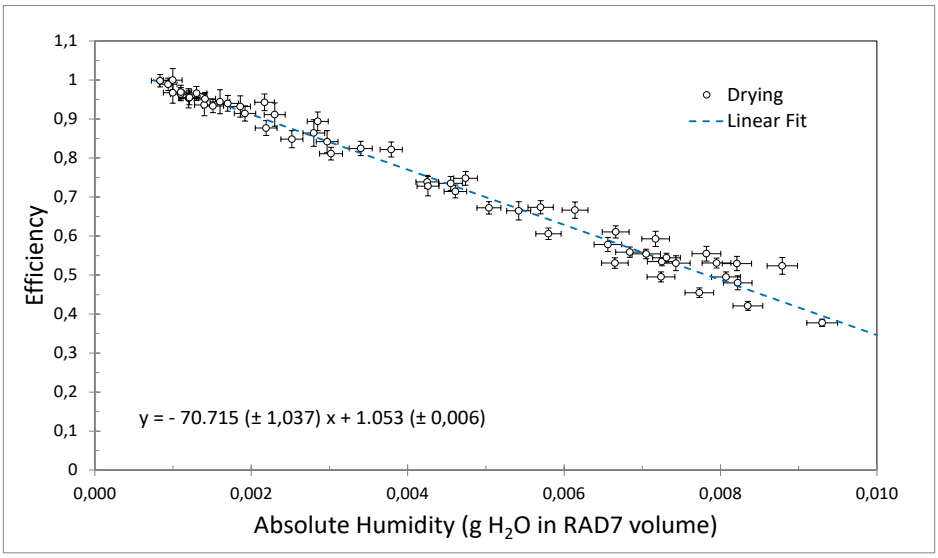

Fig. 6. Efficiency of the electrostatic collection-based silicon detectors against the water content inside RAD7. Data from the drying phases of the three different experiments up to 0.01 g of water in RAD7 volume are selected. The linear fit is reported for comparison with figures 4, 5 and 7.

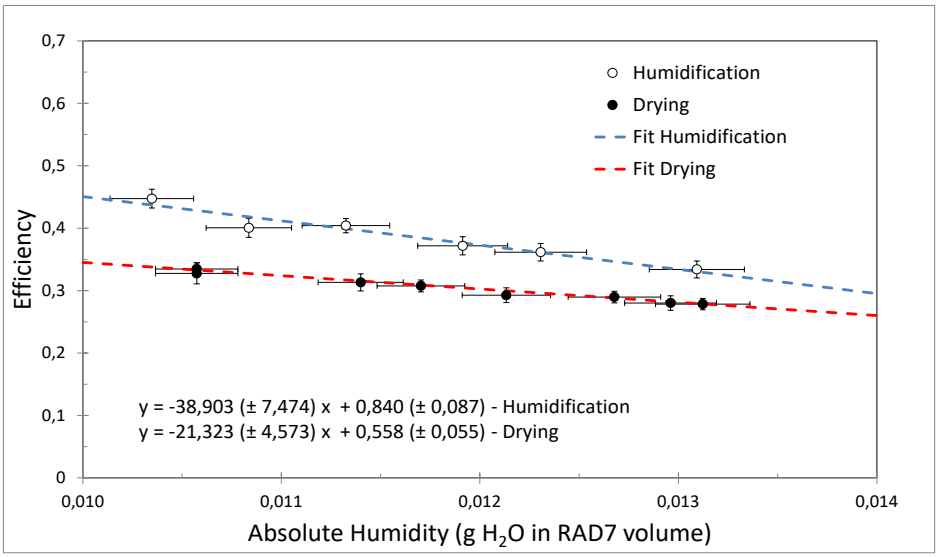

Fig. 7. Efficiency of the electrostatic collection-based silicon detectors against the water content inside RAD7. Data from the humidification and the drying phases of different experiments with more than 0.01 g of water in RAD7 volume are selected. The linear fits are reported for comparison with figures 4, 5 and 6.

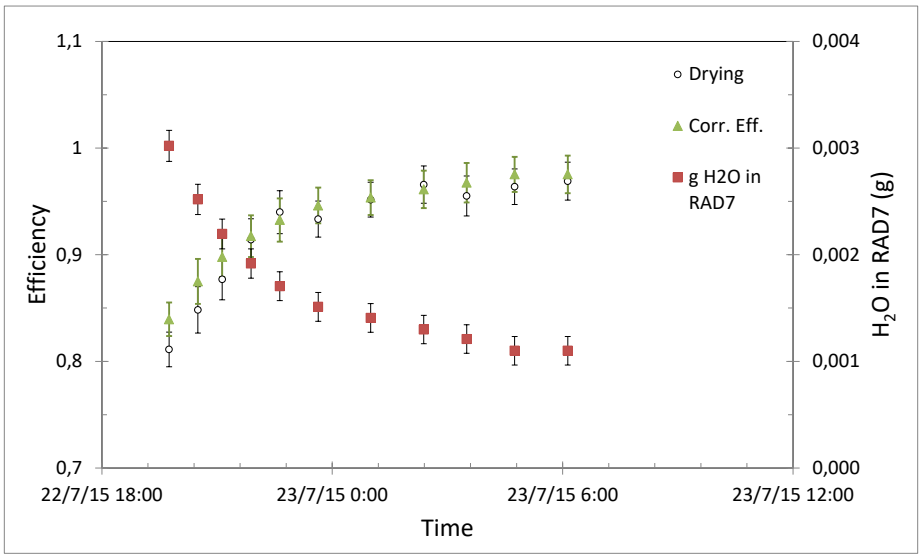

Fig. 8. Efficiency of the electrostatic collection-based silicon detectors and water content inside RAD7 overnight. Data are shown for low absolute humidity, during the drying phase. Corrected efficiency values based on linear fits in Fig. 6 (drying trend) are reported to show the effect of water-polonium clusters on the timing of efficiency recovery.

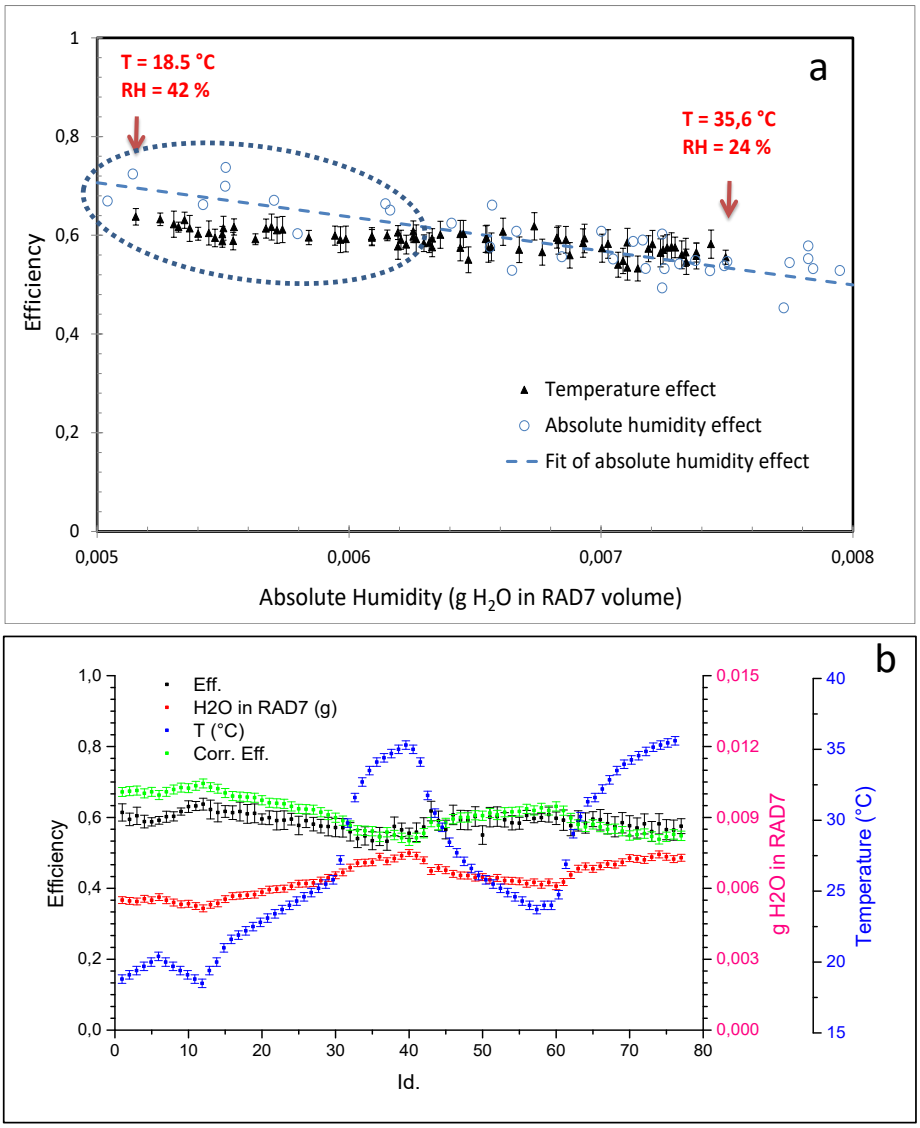

Fig. 9. Effect of changing temperature (from 18.5 to 35.6 °C) on the efficiency of the electrostatic collection-based silicon detectors. This influence is shown against the grams of water inside RAD7 (Fig. 9a). Errors are quoted as 1 sigma. A comparison with data from Fig. 4, representing the effect of absolute humidity at nearly constant temperature (26.1 ± 0.3), is shown along with relative linear fit. In Fig. 9b, the experimental efficiency is compared with the efficiency corrected for the effect of water inside RAD7 (see fit in Fig. 4) and is shown during the test (as progressive identification data) along with water and temperature changes. See text for explanation.

Table 1. Efficiency deviation of RAD7 S.N. 0608 and S.N. 2504 and Capture correction compared to RAD7 S.N. 2408 efficiency as a function of RAD7 water content.

Water (g)	Efficiency Relative Deviation			
	S.N. 2408	S.N. 0608	S.N. 2504	Capture
0,004	1,00	0,14	0,23	0,07
0,006	1,00	0,14	0,29	0,17
0,008	1,00	0,16	0,38	0,35
0,01	1,00	0,18	0,52	0,66
0,012	1,00	0,10	0,45	0,75
0,014	1,00	0,15	0,57	1,14